

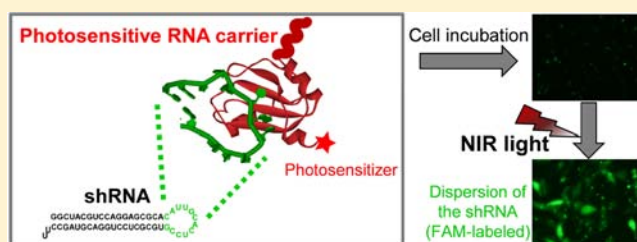
## Near-Infrared Light-Directed RNAi Using a Photosensitive Carrier Molecule

Yuka Matsushita-Ishiodori, Mika Morinaga, Kazunori Watanabe, and Takashi Ohtsuki\*

Department of Biotechnology, Graduate School of Natural Science and Technology, Okayama University, 3-1-1 Tsushimanaka, Okayama 700-8530, Japan

### S Supporting Information

**ABSTRACT:** Controlled activation of small RNAs, such as small interfering RNA, in cells is very useful for various biological applications. Light is an effective inducer of controlled activation; in particular, near-infrared light is favorable because it can penetrate deeper into tissues than UV or visible light. In this study, near-infrared light control of RNA interference (RNAi) was demonstrated in mammalian cells using a photosensitive RNA carrier molecule, consisting of an RNA carrier protein and a fluorochrome. The photosensitive carrier molecule was identified from six candidates, each with a different fluorochrome. Using this carrier molecule, cytosolic RNA delivery and RNAi can be triggered by near-infrared light. Cytotoxicity was not observed after photoinduction of RNAi.



### INTRODUCTION

Small RNAs, such as small interfering RNAs (siRNAs), short hairpin RNAs (shRNAs), and microRNAs (miRNAs), can control various cellular events. Since an siRNA or shRNA can interfere in the expression of a specific gene through the RNA interference (RNAi) mechanism, these RNAs have been widely used for functional studies of genes related to diseases, cell differentiation, embryogenesis, and apoptosis, among other applications.<sup>1–3</sup> Clinical applications of small RNAs have also been actively studied in recent years.<sup>4–6</sup> For all of these purposes, efficient and target-specific RNA delivery methods are important.

Recently, we devised a light-directed cytosolic RNA delivery method using photosensitive RNA carrier molecules.<sup>7</sup> The carrier molecules consist of a cell-permeable RNA-binding protein, such as TatU1A or FHVU1A,<sup>8</sup> and a fluorescent dye as a photosensitizer. TatU1A is a fusion protein between a TAT-derived cell-penetrating peptide (CPP)<sup>9,10</sup> and the U1A RNA-binding protein (RBP).<sup>11</sup> The photosensitive RNA carrier molecule (TatU1A-dye) can form a complex with an RNA molecule bearing a U1A binding sequence. The complexes are internalized by cells via the endocytotic pathway and entrapped in endosomes before photostimulation, while after irradiation, they are released into the cytosol. When an shRNA is used in the light-directed cytosolic RNA delivery method, gene silencing can be induced by light. This photoinduced RNAi strategy was termed CLIP-RNAi (CPP-linked RBP-mediated RNA internalization and photoinduced RNAi).

Visible light at wavelengths of 530–640 nm can be used in the light-directed cytosolic RNA delivery (or light-directed RNAi) method.<sup>12</sup> However, visible light is insufficient for *in vivo* applications because of its limited penetration into tissues.

By contrast, near-infrared (NIR) light, at around 670–880 nm, can penetrate deep into tissues.<sup>13</sup> In this study, we attempted to expand the excitation wavelength of the CLIP-RNAi method to the NIR region by examining RNA delivery using six TatU1A-dye molecules bearing a NIR fluorochrome.

### EXPERIMENTAL SECTION

**Preparation of TatU1A-Dye Molecules.** The TatU1A protein (RNA carrier protein) bearing a C-terminal Cys residue was purified as described previously.<sup>7</sup> The purified TatU1A protein (25–30  $\mu$ M) and a dye with a thiol-reactive maleimide group (50  $\mu$ M) were mixed in a buffer containing 50 mM HEPES-KOH (pH 7.5), 100 mM (NH<sub>4</sub>)<sub>2</sub>SO<sub>4</sub>, 150 mM imidazole, and 20% glycerol, and then incubated at 25 °C for 1 h. The dyes used here were DY-750 (Dyomics, Germany), Alexa Fluor 750 C<sub>5</sub> (Molecular Probes, Eugene, OR), HiLyte Fluor 750 C<sub>2</sub> (AnaSpec, Fremont, CA), DyLight 750 (Pierce, IL, USA), DyLight 800 (Pierce), and IRDye 800CW (LI-COR, NE, USA). The dye-modified TatU1A molecules (TatU1A-dye) were purified in a Centri-Sep spin column (Princeton Separations, NJ, USA) equilibrated with T buffer [20 mM HEPES-KOH (pH 7.4), 115 mM NaCl, 5.4 mM KCl, 1.8 mM CaCl<sub>2</sub>, 0.8 mM MgCl<sub>2</sub>, and 13.8 mM glucose].

Protein concentration was determined using a Protein Assay Kit (Bio-Rad, CA, USA). Labeling efficiencies of the carrier proteins were calculated by measuring the absorbance of dyes with a NanoDrop 1000 spectrophotometer (Thermo Scientific, CA, USA) (Figure S1, Supporting Information). In all

**Received:** March 4, 2013

**Revised:** July 28, 2013

**Published:** September 3, 2013



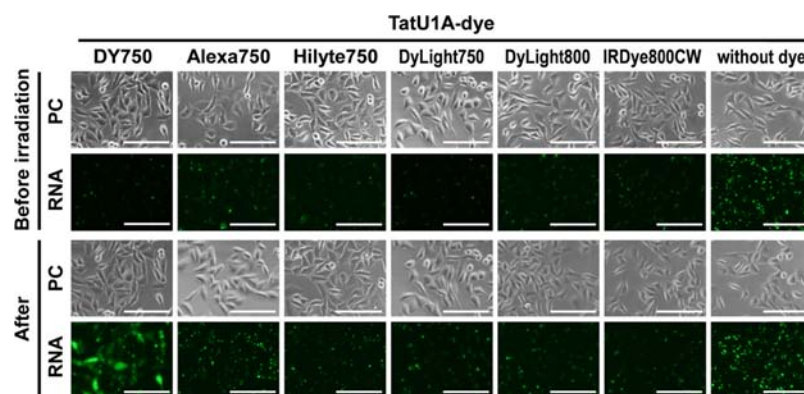


**Figure 1.** Translocation of the TatU1A-dye/shRNA complexes via endocytosis. CHO cells were treated with TatU1A-dye/shRNA-FAM complexes for 2 h at 37 °C and irradiated for 5 min at the appropriate excitation wavelengths for each dye (TatU1A-DY750, TatU1A-Alexa750, TatU1A-Hilyte750, and TatU1A-DyLight750, 735–765 nm (light source, infrared illuminator L750-66-60; Epitex Inc.); TatU1A-DyLight800 and TatU1A-Dye800CW, 760–800 nm (light source, infrared illuminator L780-66-60)). Phase contrast (PC) and shRNA images were taken before and after irradiation. Scale bar, 100  $\mu$ m.

experiments, labeling efficiencies were adjusted to 20% using separately prepared unlabeled carrier proteins.

**Preparation of shRNAs.** The shRNA sequence used was as follows: 5'-GGCUACGUCCAGGAGCGCA-CAUUGCACUCCGUCGCGUCCUGGACGUAGCCUU-3' (the U1A binding sequence is underlined). This shRNA and the 3'-FAM-labeled shRNA were purchased from JBioS (Japan).

**Cell Culture.** Chinese hamster ovary (CHO) cells and CHO cells stably expressing destabilized EGFP (EGFP-CHO) were cultured in Ham's F-12 medium (Sigma), supplemented with 10% fetal bovine serum (Biowest, France), 100 units/mL penicillin, and 100  $\mu$ g/mL streptomycin (Life Technologies, CA, USA).

**Cellular RNA Delivery by the TatU1A-Dye Molecules.** The FAM-labeled RNA (200 nM) and the carrier (2  $\mu$ M) were mixed in T buffer and incubated at 37 °C for 10 min. CHO cells were grown in 96-well plates to 70% confluence and treated for 2 h with the carrier/RNA complex described above. After washing twice with T buffer, the cells were visualized using a fluorescence microscope IX51 with a DP72 digital camera (Olympus, Japan). For endosomal escape of the carrier/RNA complex, cells were irradiated at appropriate excitation wavelengths for each dye. When using dyes with maximum excitation wavelengths close to 750 nm (DY-750, Alexa Fluor 750, HiLyte Fluor 750, and DyLight750), cells were irradiated at 735–765 nm for 5 min with an Infrared illuminator L750-66-60 (Epitex Inc., Japan) (fluence rate,  $\sim$ 150 mW/cm<sup>2</sup> on the device shown in Figure S2 (Supporting Information); total dose, 45 J/cm<sup>2</sup>). When using dyes with maximum excitation wavelengths close to 800 nm (DyLight 800 and Dye 800CW), cells were irradiated at 760–800 nm for 5 min with an Infrared illuminator L780-66-60 (Epitex Inc.) (fluence rate,  $\sim$ 190 mW/cm<sup>2</sup>; total dose, 57 J/cm<sup>2</sup>).

**Detection of Singlet Oxygen.** Singlet oxygen sensor green reagent (Molecular Probes) was used for the detection of singlet oxygen (<sup>1</sup>O<sub>2</sub>). The reagent was added at a final concentration of 1  $\mu$ M to samples containing 2  $\mu$ M TatU1A-dye in T buffer. The samples were irradiated at the appropriate excitation wavelengths for each dye, as described in Cellular RNA Delivery by the TatU1A-Dye Molecules. The measurement of green fluorescence of the sensor reagent was directly quantified using FLUOstar OPTIMA (BMG Labtech,

Germany), using 485 nm excitation and 520 nm emission filter sets.

**Induction of RNAi-Mediated EGFP Silencing and Analysis of Expression Levels of the EGFP Gene.** The unlabeled RNA (100 nM) and the carrier (2  $\mu$ M) were mixed in T buffer and incubated at 37 °C for 10 min. EGFP-CHO cells were grown in 96-well plates to 70% confluence and treated for 2 h with the unlabeled RNA/carrier complex. The RNA was delivered to the cells by the carrier, and photo-accelerated endosomal escape was induced by light at the appropriate excitation wavelengths for each dye as described in Cellular RNA Delivery by the TatU1A-Dye Molecules. Twenty hours after irradiation, cells were recovered from dishes and resuspended in PBS. EGFP mean fluorescence intensities (MFIs) were determined by flow cytometry using FACSCalibur and CellQuest software (BD Biosciences, CA, USA) as described previously.<sup>8</sup> For all experiments, data were acquired from 10,000 cells.

**Detection of Cytotoxicity.** Cytotoxicity was evaluated using the Cytotoxicity Detection kit (LDH) (Roche, Switzerland) as described previously.<sup>7</sup> At 20 h after photostimulation, an aliquot of medium was removed and mixed with the cytotoxicity detection substrate according to the manufacturer's protocol. The absorbance of the samples at 490 nm was measured, and the percent cytotoxicity for each sample was calculated from the absorbance. Values from cells incubated with medium containing 0.2% NP-40 were used as positive controls (100% cytotoxicity).

## RESULTS

**Identification of a NIR Photosensitizer for Photo-Dependent Cytosolic RNA Dispersion from among Six Fluorescent Dyes.** Six fluorescent dyes, DY-750, Alexa Fluor 750, HiLyte Fluor 750, DyLight 750, DyLight 800, and IRDye 800CW, were selected as candidate photosensitizers. The TatU1A fusion protein, which was the first RNA carrier protein designed by our group, was prepared as described above. The TatU1A proteins labeled with the above-mentioned dyes were named TatU1A-DY750, TatU1A-Alexa750, TatU1A-HiLyte750, TatU1A-DyLight750, TatU1A-DyLight800, and TatU1A-Dye800CW, respectively. The shRNA molecule containing an U1A binding sequence in its loop region was used as the cargo RNA.

We examined whether TatU1A-dye variants could carry the shRNA molecule into cells and whether photostimulation induced endosomal escape of the TatU1A-dye/shRNA complexes. To visualize localization of the shRNA, we used FAM-labeled shRNAs. In all cases, FAM fluorescence signals appeared as small particles in the cells before irradiation, indicating that the TatU1A-dye/shRNA complexes were trapped in endosomes (Figure 1), as previously reported.<sup>7</sup> As clearly shown in Figure 1, when the TatU1A protein labeled with DY-750 was used as a carrier, FAM fluorescence signals were dispersed throughout the cytosol after irradiation at 735–765 nm. A similar result was observed in the presence of 5% serum (50  $\mu$ L of T buffer containing TatU1A-DY750/shRNA was added to cells cultured in 50  $\mu$ L of F12 medium containing 10% fetal bovine serum); however, cells needed to be treated for a longer time (3–4 h) for the shRNA to be efficiently delivered. By contrast, the other cases showed no changes in FAM fluorescence signals after irradiation at the appropriate excitation wavelengths for each dye.

**Detection of Singlet Oxygen Generation.** It has been reported that photosensitizers generate reactive oxygen species, presumably singlet oxygen ( $^1\text{O}_2$ ), in a light-dependent manner, leading to disruption of the endocytic vesicle and release of target molecules to the cytosol. We thus examined if the above-mentioned candidate photosensitizers generated singlet oxygen. The singlet oxygen sensor green reagent, which emits a green fluorescence in the presence of singlet oxygen, was added to samples containing 2  $\mu$ M TatU1A-dye in T buffer, and these were irradiated at the appropriate excitation wavelengths for each dye. After irradiation, the measurements of green fluorescence of the sensor reagent were quantified. As shown in Figure 2, in the case of TatU1A protein labeled with DY-750, singlet oxygen generation was clearly detected. By contrast, the generation of singlet oxygen from the other TatU1A-dyes was barely detectable in comparison with that in TatU1A-DY750.

**RNAi Can Be Induced with TatU1A-DY750 Using NIR Light.** The efficiency of RNAi photoinduction using TatU1A-DY750 was investigated by measuring EGFP knockdown

efficiency in EGFP-CHO cells. EGFP silencing at 20 h after photostimulation was assessed by flow cytometry. Treatment with TatU1A-DY750/shRNA(anti-EGFP) complexes induced a dramatic reduction in EGFP MFI in a light-dependent manner (Figure 3a). The treatment of cells with the TatU1A-DY750/shRNA complex followed by photostimulation led to a 70% reduction in MFI, compared with control cells treated with T buffer in the absence of the carrier/shRNA complex (Figure 3b). A similar knockdown efficiency was observed when EGFP-CHO cells were transfected with anti-EGFP siRNA using the TransIT-TKO transfection reagent (Mirus).<sup>7</sup> By contrast, no decrease in MFI was observed in cells treated with the TatU1A-Alexa750/shRNA complex (Figure 3a,b). These data indicate that the TatU1A-DY750 can act as a photosensitive carrier in this photoinducible RNAi method using NIR light.

**Treatment with the TatU1A-DY750/shRNA Complex Followed by Photostimulation Did Not Result in Cytotoxicity.** In parallel with RNAi evaluation, we also investigated cytotoxicity. No cytotoxicity was observed under the conditions of these experimental conditions, either with or without photostimulation (Figure 4). These data suggest that the cells treated with the TatU1A-DY750/shRNA complex were not damaged by photostimulation.

## DISCUSSION

Our previous report showed that visible light at wavelengths of 530–640 nm, which is less toxic than UV light, can be used for photoinduction of RNAi;<sup>12</sup> however, visible light is unsuitable for use *in vivo* because of its limited penetration into tissues. In this study, we demonstrate the induction of RNAi using NIR light at  $\sim 750$  nm, which is able to penetrate deep into tissues.

In this study, six fluorescent dyes, all having absorption maxima in the NIR region, were chosen as candidate photosensitizers. All six dyes had a maleimide group, facilitating attachment of the thiol group of the TatU1A protein, which contained a C-terminal Cys residue. All of the TatU1A-dye molecules included in this study were capable of carrying the target shRNA into cellular endosomes (Figure 1, before irradiation). The observation that shRNA-FAM fluorescent signals were weaker in cells containing TatU1A-dyes than in those with unlabeled TatU1A may be due to fluorescence resonance energy transfer between FAM and the NIR fluorescent dye. Interestingly, among six candidates, only TatU1A labeled with DY-750 possessed the ability to escape photo-dependently from endosomes (Figure 1; after irradiation). As the chemical structures of the dyes used, other than those of DY-750 and IRDye 800CW, are unknown, we are unable to relate these to the differences observed in photo-dependent endosomal escape. The molar extinction coefficients of these dyes all fall within a narrow range (210000–275000  $\text{M}^{-1}\text{cm}^{-1}$  at  $\sim 770$  nm for DyLight 800 and IRDye 800CW, and at  $\sim 750$  nm for the other four dyes), suggesting that these coefficients do not contribute significantly to endosomal escape. The phenomenon of endosomal escape (Figure 1) is likely to be related to the light-dependent generation of  $^1\text{O}_2$  in solutions containing TatU1A-dyes (Figure 2); substantial  $^1\text{O}_2$  generation was observed only in TatU1A-DY750 solution but scarcely in other TatU1A-dye solutions. These data suggest that photo-dependent  $^1\text{O}_2$  generation from the photosensitizer DY-750 induces disruption of the endocytic vesicle, leading to the release of RNA to the cytosol.

NIR light-dependent RNAi using TatU1A-DY750 was demonstrated by evaluation of EGFP silencing in targeted

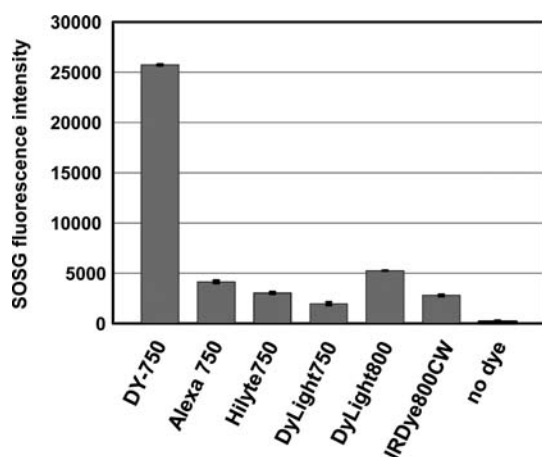


**Figure 2.** Measurement of singlet oxygen generation. The Singlet Oxygen Sensor Green reagent (Molecular Probes) (1  $\mu$ M) and TatU1A-dye (2  $\mu$ M) were mixed in T buffer and irradiated at the appropriate excitation wavelengths for each dye, as described in the legend to Figure 1. Fluorescence intensities were measured using a spectrofluorometer (FLUOstar OPTIMA; BMG Labtech), with a 485 nm excitation and 520 nm emission filter set. Data represent means with error bars displaying maximum and minimum values,  $n = 2$ .



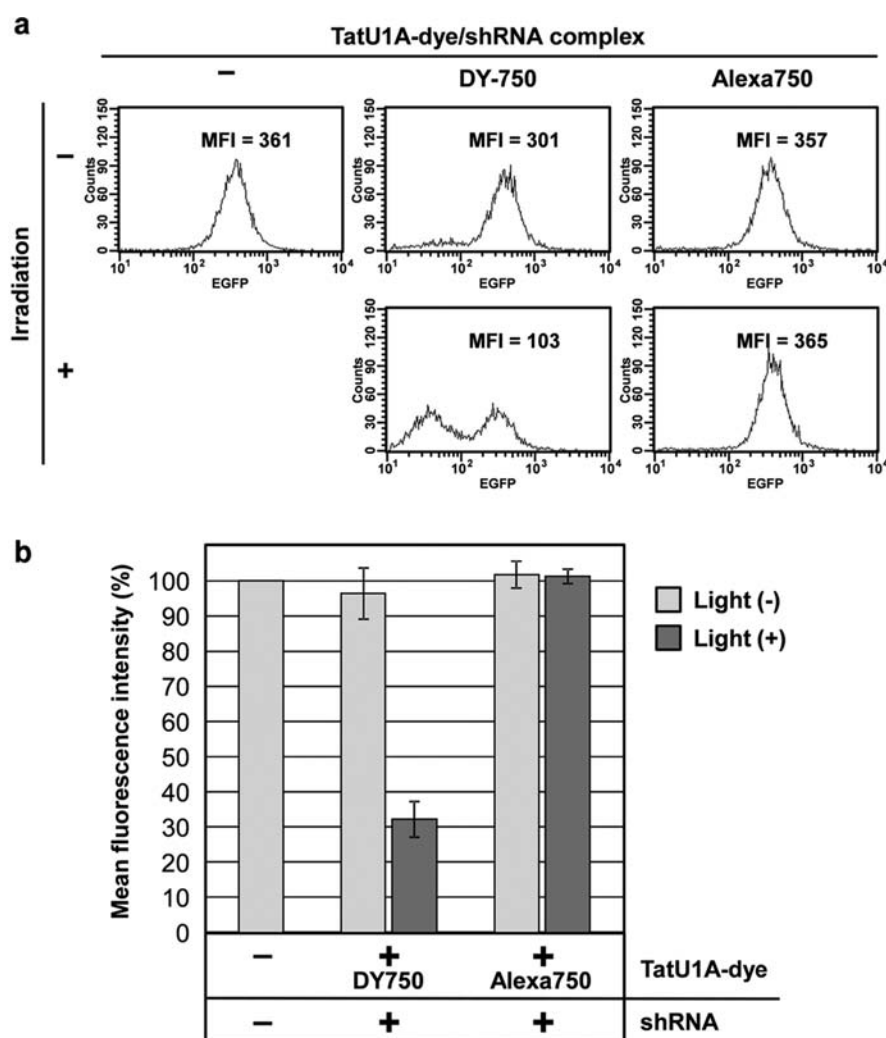


**Figure 3.** EGFP silencing by TatU1A-dye/shRNA complexes. The shRNAs, which contain both anti-GFP and U1A-binding sequences, were delivered into EGFP-CHO cells. (a) Flow cytometric analysis of EGFP-expressing cells treated with TatU1A-dye/shRNA complexes and irradiated (735–765 nm for 5 min). Cells were collected for flow cytometric analysis at 20 h after irradiation. Silencing was assessed by measuring EGFP mean fluorescence intensity (MFI). (b) Comparison of TatU1A-dye molecules in EGFP silencing. EGFP MFIs of cells treated with different TatU1A-dye/shRNA complexes are compared to control cells treated with T buffer only. Data represent the means  $\pm$  SD,  $n = 4$ .

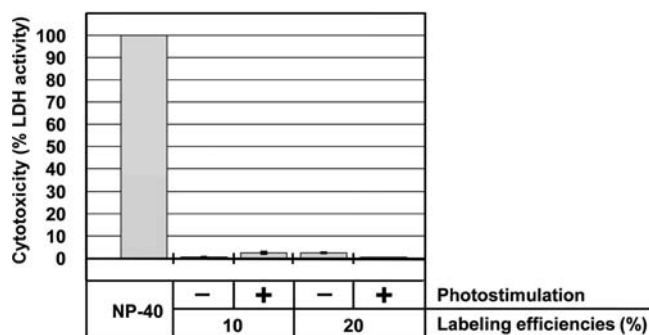


**Figure 4.** Cytotoxicity after treatment with the TatU1A-DY750/shRNA complex followed by photostimulation. Cellular RNA delivery using TatU1A-DY750 was carried out as described in the legend to Figure 3. At 20 h after treatment with the TatU1A-DY750/shRNA complex followed by photostimulation, cytotoxicity was evaluated using the Cytotoxicity Detection kit (LDH) (Roche). The values for cells incubated with medium containing 0.2% NP-40 were used as a positive control (100% cytotoxicity). Data represent the means  $\pm$  SD,  $n = 3$ .

cells. The treatment of cells with the TatU1A-DY750/shRNA(anti-EGFP) complex, followed by photostimulation, resulted in a 70% reduction in EGFP expression, compared with control cells treated with buffer lacking the TatU1A-DY750/shRNA complex (Figure 3). These data indicate that TatU1A-DY750 can act as a photosensitive carrier in the CLIP-RNAi method using NIR light. It should be noted that TatU1A-DY750 itself may have endosomal escape ability, as a slight EGFP knockdown was observed in cells treated with TatU1A-DY750/shRNA complexes, even in the absence of photostimulation (Figure 3b; reproducible result). TatU1A-Alexa750 (Figure 3b), TatU1A-Alexa546, and several other photosensitive molecules previously studied<sup>8</sup> did not induce RNAi after shRNA treatment in the absence of photostimulation.

For fine control of RNAi on the microscale, light is a favorable inducer. Several groups have reported strategies for photoinduced RNAi, including the caged siRNA strategy, photochemical internalization (PCI), and photothermal transfection.<sup>14–17</sup> Specifically, some recent reports demonstrated NIR light-dependent RNAi based on photothermal transfection using a 800 nm laser,<sup>17</sup> 800 nm laser-triggered siRNA release

from a gold nanoshell,<sup>18,19</sup> upconversion nanoparticles (UCNs) modified with cationic photocaged linkers connecting the particles with siRNAs, which can be released by 980 nm light,<sup>20</sup> and UCNs carrying caged siRNAs that can be uncaged by 980 nm light.<sup>21</sup> The leakage RNAi activity of TatU1A-DY750 in nonirradiated cells was less than 4% (Figure 3b), which is lower than that of the gold nanoshell.<sup>19</sup> Leakage activities have not been reported in other studies of NIR-induced RNAi.<sup>17,18,20,21</sup> In contrast to the work described here, all previous investigations used gold nanoparticles or nanoshells as the RNA carrier.

## CONCLUSIONS

We have demonstrated 750 nm NIR light-directed cytosolic RNA delivery and gene silencing using a CLIP-RNAi strategy. The extension of light-triggered RNAi methods to the NIR spectral region will facilitate studies of gene function *in vivo* and the development of new therapeutic approaches.

## ASSOCIATED CONTENT

### Supporting Information

UV-vis spectra of TatU1A-DY750 and TatU1A protein; irradiation device for NIR light-stimulation of cells; and flow cytometric analysis of EGFP-expressing cells treated with TatU1A/shRNA complexes and irradiated. This material is available free of charge via the Internet at <http://pubs.acs.org>.

## AUTHOR INFORMATION

### Corresponding Author

\*Tel: +81-86-251-8218. E-mail: [ohtsuk@okayama-u.ac.jp](mailto:ohtsuk@okayama-u.ac.jp).

### Notes

The authors declare no competing financial interest.

## ACKNOWLEDGMENTS

We thank Dr. M. Magari and Professor H. Ohmori (Okayama University) for their support with the flow cytometric analysis. This work was supported by Grant-in-Aid for Young Scientists (A) and Grant-in-Aid for Scientific Research on Innovative Areas "Nanomedicine Molecular Science" from MEXT, Japan.

## REFERENCES

- (1) Sims, D., Mendes-Pereira, A. M., Frankum, J., Burgess, D., Cerone, M. A., Lombardelli, C., Mitsopoulos, C., Hakas, J., Murugesu, N., Isacke, C. M., Fenwick, K., Assiotis, I., Kozarewa, I., Zvelebil, M., Ashworth, A., and Lord, C. J. (2011) High-throughput RNA interference screening using pooled shRNA libraries and next generation sequencing. *Genome Biol.* 12, R104.
- (2) Yau, W. W., Rujitanaroj, P. O., Lam, L., and Chew, S. Y. (2012) Directing stem cell fate by controlled RNA interference. *Biomaterials* 33, 2608–2628.
- (3) Tenlen, J. R., McCaskill, S., and Goldstein, B. (2013) RNA interference can be used to disrupt gene function in tardigrades. *Dev. Genes Evol.* 223, 171–181.
- (4) Burnett, J. C., and Rossi, J. J. (2012) RNA-based therapeutics: current progress and future prospects. *Chem. Biol.* 19, 60–71.
- (5) Kole, R., Krainer, A. R., and Altman, S. (2012) RNA therapeutics: beyond RNA interference and antisense oligonucleotides. *Nat. Rev. Drug Discovery* 11, 125–140.
- (6) Nana-Sinkam, S. P., and Croce, C. M. (2012) Clinical applications for microRNAs in cancer. *Clin. Pharmacol. Ther.* 93, 98–104.
- (7) Endoh, T., Sisido, M., and Ohtsuki, T. (2008) Cellular siRNA delivery mediated by a cell-permeant RNA-binding protein and photoinduced RNA interference. *Bioconjugate Chem.* 19, 1017–1024.
- (8) Matsushita-Ishiodori, Y., Kuwabara, R., Sakakoshi, H., Endoh, T., and Ohtsuki, T. (2011) Photosensitizing carrier proteins for photoinducible RNA interference. *Bioconjugate Chem.* 22, 2222–2226.
- (9) Gump, J. M., and Dowdy, S. F. (2007) TAT transduction: the molecular mechanism and therapeutic prospects. *Trends Mol. Med.* 13, 443–448.
- (10) Endoh, T., and Ohtsuki, T. (2009) Cellular siRNA delivery using cell-penetrating peptides modified for endosomal escape. *Adv. Drug Delivery Rev.* 61, 704–709.
- (11) Oubridge, C., Ito, N., Evans, P. R., Teo, C. H., and Nagai, K. (1994) Crystal structure at 1.92 Å resolution of the RNA-binding domain of the U1A spliceosomal protein complexed with an RNA hairpin. *Nature* 372, 432–438.
- (12) Endoh, T., Sisido, M., and Ohtsuki, T. (2009) Spatial regulation of specific gene expression through photoactivation of RNAi. *J. Controlled Release* 137, 241–245.
- (13) Weissleder, R. (2001) A clearer vision for *in vivo* imaging. *Nat. Biotechnol.* 19, 316–317.
- (14) Matsushita-Ishiodori, Y., and Ohtsuki, T. (2012) Photoinduced RNA interference. *Acc. Chem. Res.* 45, 1039–1047.
- (15) Casey, J. P., Blidner, R. A., and Monroe, W. T. (2009) Caged siRNAs for spatiotemporal control of gene silencing. *Mol. Pharmaceutics* 6, 669–685.
- (16) Oliveira, S., Hogset, A., Storm, G., and Schifflers, R. M. (2008) Delivery of siRNA to the target cell cytoplasm: photochemical internalization facilitates endosomal escape and improves silencing efficiency, *in vitro* and *in vivo*. *Curr. Pharm. Des.* 14, 3686–3697.
- (17) Lu, W., Zhang, G., Zhang, R., Flores, L. G., II, Huang, Q., Gelovani, J. G., and Li, C. (2010) Tumor site-specific silencing of NF- $\kappa$ B p65 by targeted hollow gold nanosphere-mediated photo-thermal transfection. *Cancer Res.* 70, 3177–88.
- (18) Braun, G. B., Pallaoro, A., Wu, G., Missirlis, D., Zasadzinski, J. A., Tirrell, M., and Reich, N. O. (2009) Laser-activated gene silencing via gold nanoshell-siRNA conjugates. *ACS Nano* 3, 2007–2015.
- (19) Huschka, R., Barhoumi, A., Liu, Q., Roth, J. A., Ji, L., and Halas, N. J. (2012) Gene silencing by gold nanoshell-mediated delivery and laser-triggered release of antisense oligonucleotide and siRNA. *ACS Nano* 6, 7681–7691.
- (20) Yang, Y., Liu, F., Liu, X., and Xing, B. (2012) NIR light controlled photorelease of siRNA and its targeted intracellular delivery based on upconversion nanoparticles. *Nanoscale* 5, 231–238.
- (21) Jayakumar, M. K., Idris, N. M., and Zhang, Y. (2012) Remote activation of biomolecules in deep tissues using near-infrared-to-UV upconversion nanotransducers. *Proc. Natl. Acad. Sci. U.S.A.* 109, 8483–8488.